Econ. Environ. Geol.
Vol. 30, No. 6, p. 505-517, 1997.

Fluid Inclusion and Stable Isotope Studies of the Kwangsin Pb-Zn Deposit

Kwang-Jun Choi*, Seong-Taek Yun and Chil-Sup So****

ABSTRACT : Lead and zinc mineralization of the Kwangsin mine was formed in quartz and carbonate veins that filled fault-related fractures in the limestone-rich Samtaesan Formation of the Chosun Supergroup and the phyllite-rich Suchangni Formation of unknown age. A K-Ar date of alteration sericite indicates that the Pb-Zn mineralization took place during Late Cretaceous (83.5 Ma), genetically in relation to the cooling of the nearby Muamsa Granite (83~87 Ma). Mineral paragenesis can be divided into three stages (I, II, III): (I) the deposition of barren massive white quartz, (II) the main Pb-Zn mineralization with deposition of white crystalline quartz and/or carbonates (rhodochrosite and dolomite), and (III) the deposition of post-ore barren calcite. Mineralogic and fluid inclusion data indicate that lead-zinc minerals in middle stage II (IIb) were deposited at temperatures between 182° and 276°C from fluids with salinities of 2.7 to 5.4 wt. % equiv. NaCl and with log fs_2 values of -15.5 to -11.8 atm. The relationship between homogenization temperature and salinity data indicates that lead-zinc deposition was a result of fluid boiling and later meteoric water mixing. Ore mineralization occurred at depths of about 600 to 700 m. Sulfur isotope compositions of sulfide minerals ($\delta^{34}S_{CDT}$=9.0~14.5 ‰) indicate a relatively high $\delta^{34}S_{\Sigma S}$ value of ore fluids (up to 14 ‰), likely indicating an igneous source of sulfur largely mixed with an isotopically heavier sulfur source (possibly sulfates in surrounding sedimentary rocks). There is a remarkable decrease of calculated $\delta^{18}O$ value of water in hydrothermal fluids with increasing paragenetic time: stage I, 14.6~10.1 ‰; stage IIa, 5.8~2.2 ‰; stage IIb, 0.8~-2.0 ‰; stage IIc, -6.1~-6.8 ‰. This indicates a progressive increase of meteoric water influx in the hydrothermal system at Kwangsin. Measured and calculated hydrogen and oxygen isotope values indicate that the Kwangsin hydrothermal fluids was formed from a circulating (due to intrusion of the Muamsa Granite) meteoric waters which evolved through interaction mainly with the Samtaesan Formation ($\delta^{18}O$=20.1 to 24.9 ‰) under low water/rock ratios.

INTRODUCTION

The Kwangsin Pb-Zn mine is located approximately 130 km southeast of Seoul within the Hwanggangri mineralized district of the Ogcheon belt. The Hwanggangri district contains numerous mineral deposits including at least 60 W-Mo- and Cu-Pb-Zn (-Au-Ag)-bearing metallic ore deposits and lesser fluorite and talc deposits (So, Yun, 1992). Most metallic ore deposits in the district are located around the Wolagsan, Muamsa and Susan Granites of late Cretaceous age, suggesting a genetic tie between ore mineralization and granitic magmatism. The Kwangsin mine is spatially related with the Muamsa Granite (age=83± 5 Ma; So, Yun, 1992) intruding the carbonate-rich sedimentary rocks of early Paleozoic age and phyllite of unknown age, locally metamorphosing them to calc-silicate rocks. Average ore grades range from 3.1 to 13.2 wt. % lead+zinc (Kim, Kim, 1980).

This study documents the age and nature of ore mineralization and elucidates the origin and geochemical environments of ore-forming fluids.

GENERAL GEOLOGY

Geology of the mine area is composed of the Ordovician sedimentary rocks of the Chosun Supergroup, age-unknown rocks, and late Cretaceous Muamsa Granite (Kim *et al.*, 1967), as shown in Fig. 1.

The sedimentary rocks of the Chosun Supergroup are largely composed of limestones, limesilicates and hornfels, and belong to the Samtaesan Formation. Limestones generally strike N10° to 50° W and dip 40° to 80° SW and NE, and pale to dark gray in color. Silicified limestones occur along the contact with granite, and are composed of calcite and quartz with minor amounts of sericite, muscovite, biotite and magnetite.

The age-unknown metasedimentary rocks in the mine area are composed of the Keumsusan quartzite and the Suchangni Formation. The Keumsusan quart-

* Center for Mineral Resources Research, Korea University, Seoul 136-701, Korea.
** Department of Earth and Environmental Sciences, Korea University, Seoul 136-701, Korea.

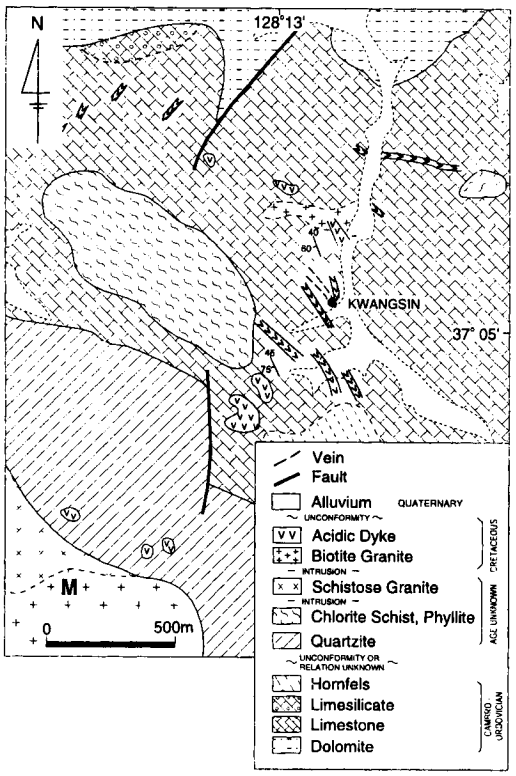

Fig. 1. Detailed geologic map of the Kwangsin mine area. M=Muamsa Granite.

zite disconformably overlies the Samtaesan Formation rocks and is intruded by the Muamsa Granite. The Suchangni Formation overlies the Samtaesan Formation rocks and consists of chlorite schist and phyllite.

The Muamsa Granite forms a small cupola which intrudes the Samtaesan Formation (Fig. 1). The granite is typically medium-grained, but its marginal portions are fine-grained with feldspar phenocrysts displaying myrmekitic and perthitic intergrowths. In the margin of the intrusion, small (< 3 mm) miarolitic cavities are often present. These textural features indicate the water-rich character of the granitic magma. The water-rich fluid could exsolve and migrate during cooling of the granite (So, Yun, 1992), which might have led to the formation of hydrothermal ore deposits. In fact, more than 50 mineral deposits (including W-Mo, Pb-Zn-Cu, fluorite and talc deposits) are concentrated around the Muamsa Granite (Kim, Shin, 1990).

The Muamsa Granite has the petrochemical characteristics of K-rich, magnetite series, I-type (or A-type) granitoids that was highly evolved through fractional crystallization of calc-alkaline magmas (So, Yun, 1992). A Rb-Sr two-point isochron age of the granite is 83±5 Ma (Table 1). Acidic dikes of granite porphyry, aplite and quartz porphyry ubiquitously intrude the Samtaesan Formation and the Keumsusan quartzite.

ORE VEINS

The Pb-Zn mineralization of the Kwangsin mine occurs as hydrothermal quartz and carbonate veins which filled fault-related fissures in the limestone-rich Samtaesan Formation and the phyllite-rich Suchangni Formation (Fig. 1). The veins are commonly parallel to the strike direction of host rocks, and generally strike N30°~40° W and dip near-vertically. Ore bodies typically occur as pockets and lenses which are about 10~15 m wide and 50 m long and extend to 250 m below the land surface. The veins locally show a spatial contact with dikes of quartz porphyry which strike N20°~50° W, probably indicating that ore mineralization was genetically related with the dike intrusion.

Mineralogy of hypogene ores is relatively simple,

Table 1. Radiometric age data for the Kwangsin Pb-Zn mine area

Sample No.	Description	K (wt. %)	Radiogenic ^{40}Ar (10^{-6}cc STP/g)	Nonradiogenic Ar (%)	Date (Ma±σ)
K-1	Sericite from alteration halo	7.66±0.15	2538.5±26.3	3.7	83.5±1.8

Rb-Sr data: two-point isochron

						Isochron parameters[1]		
	Description	^{86}Sr (ppm)	^{87}Rb (ppm)	$^{87}Sr/^{86}Sr$	$^{87}Rb/^{86}Sr$	Slope ($\times 10^{-3}$)	Intercept	Date (Ma±1σ)
GS-861[2]	Muamsa Granite							
	Whole-rock	3.05	113	0.7603	36.6	1.18(7)	0.7173(16)	83.0±5.0
	Biotite	1.145	558	1.284	482			

[1] Number in parentheses is uncertainty in the last decimal place of the slope or intercept. [2]Data from So, Yun (1992).

and consists of quartz and carbonates (rhodochrosite, dolomite and calcite) with subordinate ore minerals including galena, sphalerite, chalcopyrite, arsenopyrite, pyrite, pyrrhotite, pyrargyrite, argentite, stannite and tetrahedrite-tennantite.

Hydrothermal alteration zones characterized by sericitization and strong pyritization occur in impure limestones. Sericite from alteration haloes near veins yielded a K-Ar date of 83.5±1.8 Ma (Table 1), indicating that hydrothermal vein mineralization at Kwangsin was formed during the cooling of the Late Cretaceous Muamsa Granite (83~87 Ma).

MINERALOGY AND PARAGENESIS

Based on textural relationships and mineral assemblages, the vein mineralization at Kwangsin can be divided into three distinct paragenetic stages (Fig. 2). During stage I, massive, white-colored barren quartz veins have formed prior to main ore deposition. In stage II, quartz and carbonate (rhodochrosite, dolomite and calcite) veins with sphalerite, galena, arsenopyrite, pyrite and small amounts of chalcopyrite, pyrrhotite, marcasite, stannite, tetrahedrite-tennantite, argentite and pyrargyrite were deposited. Stage III represents a postore, milky-colored carbonate veins containing rare amounts of sulfide minerals.

Based on the spatial and temporal variation of characteristic mineral assemblages, stage II mineralization can be further divided into three substages (IIa, IIb and IIc), as described below.

Substage IIa: The substage IIa mineralization is characterized by the deposition of rhodochrosite, dolomite and quartz with minor amounts of sulfides (Fig. 2). Rhodochrosite is most abundant and usually occurs as fine-grained beige to pink-colored aggregates. Quartz occurs as white-colored aggregates which are intergrown with rhodochrosite. Fine-grained euhedral pyrite is disseminated within rhodochrosite. Sphalerite (14.8~16.0 mole % FeS; Fig. 3) is intergrown with pyrite, and shows a concentric zoning in doubly polished thin section. Arsenopyrite (29.5 to 30.6 atom. % As) occurs as euhedral to subhedral grains associated with chalcopyrite within fractures of sphalerite, and shows a slight decrease in As content from center to margin in a single grain (from 30.6 to 29.7 atom. % As). Galena occurs not only as anhedral grains filling the cracks of other sulfides but also as isolated coarse-grained euhedral crystals. Sericite-rich rock fragments occur within the stage IIa to early IIb vein portions.

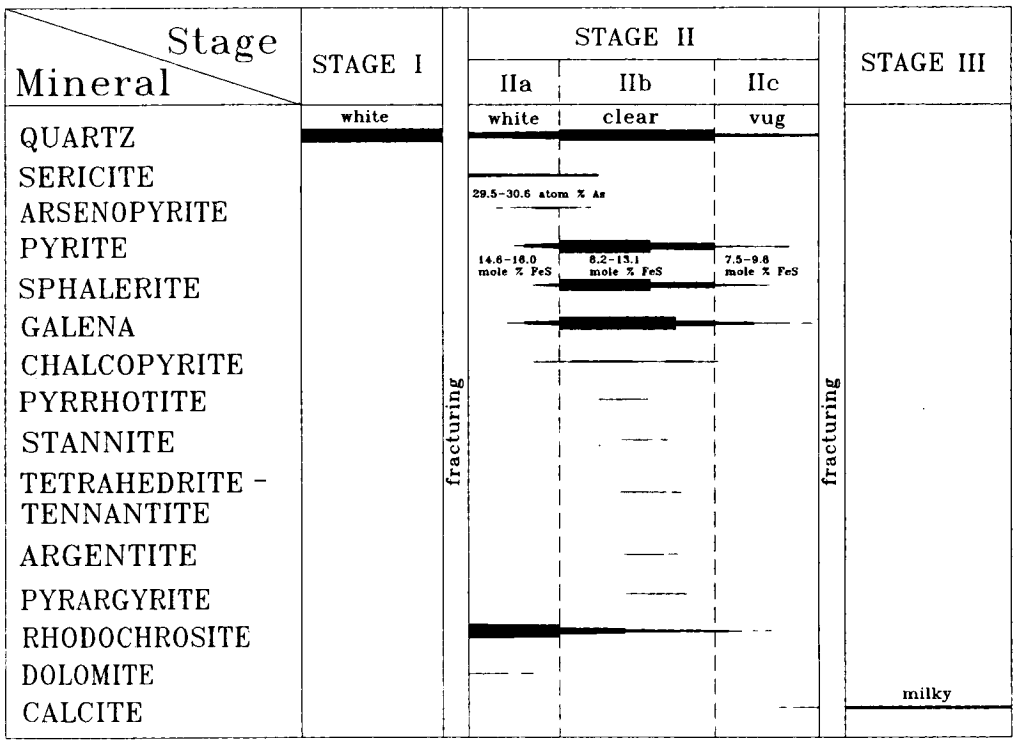

Fig. 2. Generalized paragenetic sequence of hypogene minerals from the Kwangsin mine. Width of lines corresponds to relative abundance.

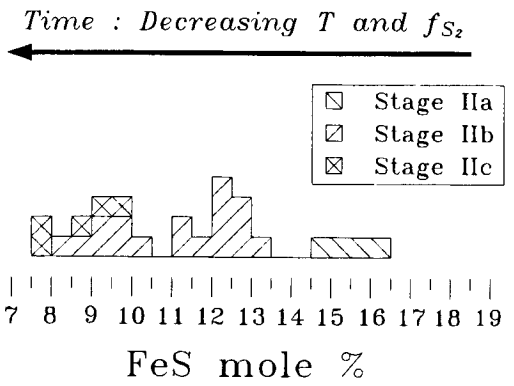

Fig. 3. FeS content of sphalerite from stage II veins of the Kwangsin mine.

Substage IIb: This substage contains all of the economic Pb-Zn mineralization. Primary minerals consist mainly of clear to milky quartz with abundant ore minerals including sphalerite, galena, pyrite and rare amounts of chalcopyrite, pyrrhotite, stannite, tetrahedrite-tennantite, pyrargyrite and argentite. Quartz usually occurs as medium-sized grains which show a comb structure. Pyrite occurs as both finely crystalline aggregates and euhedral to subhedral grains (up to 10 mm) disseminated throughout the vein. Sphalerite (8.2 to 13.1 mole % FeS; Fig. 3) forms subhedral to anhedral grains which are intergrown with chalcopyrite, galena, pyrrhotite and pyrite, and contains inclusions of chalcopyrite (as an exsolved phase), pyrrhotite and galena. Later chalcopyrite infills interstices of sphalerite and galena. Arsenopyrite forms euhedral to subhedral grains that are replaced by sphalerite. Pyrargyrite, tetrahedrite-tennantite, stannite and argentite occur as anhedral inclusions in galena.

Substage IIc: Substage IIc mineralization is characterized by the deposition of clear quartz and beige-colored rhodochrosite in vugs. The quartz and rhodochrosite form euhedral crystals up to 10 mm and 2 mm in length, respectively. Ore minerals are mainly pyrite and rare amounts of sphalerite (7.5 to 9.8 mole % FeS) and galena.

FLUID INCLUSION STUDIES

Fluid inclusions were examined in 51 representative samples of quartz and carbonates from veins and of quartz from pegmatitic portions in the Muamsa Granite, in order to determine the temporal and spatial variations in temperature and composition of the hydrothermal fluids.

Microthermometric measurements were made on a U.S.G.S./Fluid Inc. gas-flow heating-freezing system.

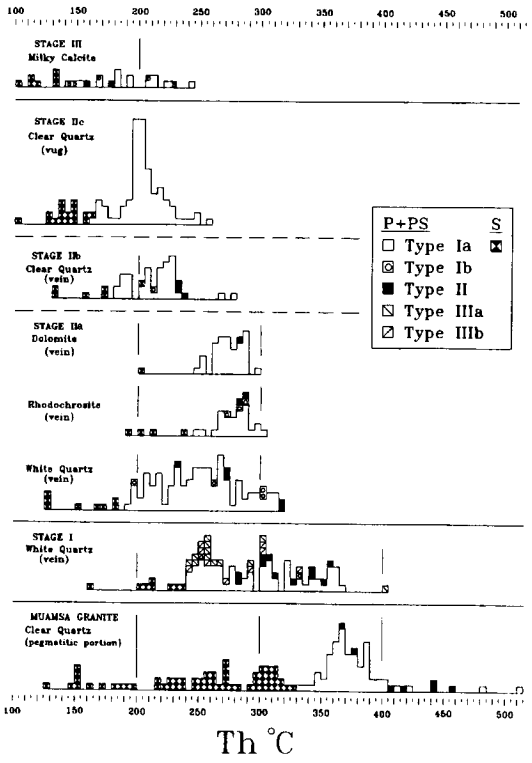

Fig. 4. Frequency diagrams of homogenization temperature of fluid inclusions in vein minerals from the Kwangsin mine. Homogenization temperatures of fluid inclusions in clear quartz from pegmatitic portion of the Muamsa Granite are also shown. See text for the classification scheme of fluid inclusion types. P+PS=primary+pseudosecondary, S=secondary.

Salinity data reported are based on freezing point depression in the system H_2O-NaCl (Bodnar, 1993) for CO_2-absent aqueous inclusions, and on clathrate-melting temperatures (Bozzo *et al.*, 1975; Diamond, 1992) for CO_2-bearing inclusions. Results of heating and freezing experiments are shown in Fig. 4 to 6.

Types of Fluid Inclusions

Three main types of fluid inclusions were observed and are classified herein based on phase relations at room temperature or during freezing runs: type I (liquid-rich, aqueous), type II (vapor-rich, aqueous) and type III (liquid CO_2-bearing). The order of abundance is type I > type II > type III. The inclusions are generally less than 20 μm in size (max. 90 μm in substage IIc vug quartz). The principal fluid inclusion types are described as follows.

Type I fluid inclusions are the predominant type

and contain a gas bubble comprising 5 to 40 vol. percent of the total inclusion volume at room temperature. Type I inclusions occur as primary, pseudosecondary and secondary inclusions, with variable size from < 5 to 40 μm (usually 10~20 μm). They are readily homogenized to the liquid phase upon heating and do not contain daughter minerals. Type I inclusions can be divided into two subtypes: Ia and Ib. The bubbles of type Ia inclusions appear to be essentially water vapor. Type Ib inclusions recognizably formed the CO_2 gas hydrate ($CO_2 \cdot 5.75\ H_2O$) during freezing runs, indicating that minor amounts of CO_2 ($\approx$0.85 molal, the level required for CO_2 clathrate formation; Hedenquist, Henley, 1985) are contained in these inclusions.

Type II fluid inclusions are water vapor-rich (60~90 vol. percent of the total inclusion volume) at room temperature. Neither liquid CO_2 nor CO_2 clathrate was detected optically in these inclusions during freezing experiment. Type II inclusions are observed only as primary and pseudosecondary inclusions and homoge- nize to the vapor phase upon heating. They are gene- rally small in size (3 to 6 μm), and therefore it was difficult to estimate the salinity of type II inclusion.

Type III fluid inclusions contain three phases (liquid CO_2, gas CO_2, and an aqueous liquid) at room temperature. They occur in stage I quartz as primary inclusions (< 10~30 μm, usually 15~25 μm in size). The volumetric ratio of CO_2 (liquid+vapor) to aqueous liquid varies within the range 85:15 to 5:95. According to the mode of total homogenization, type III inclusions can be further divided into two subtypes: type IIIa and type IIIb. Type IIIa inclusions are more common and homogenize totally to the H_2O-rich phase (if they do not decrepitate upon heating). Type IIIb inclusions homogenize to the CO_2 -rich phase but usually decrepitate on heating due to the build-up of high internal pressures.

Microthermometric Data

Inclusions in the Muamsa granite

Primary-like inclusions in clear quartz from pegmatitic portions of the Muamsa Granite are the type Ia and type II inclusions which homogenize at temperatures from 334° to 513°C and 362° to 457°C, respectively. Type I inclusions have salinities of 7.0 to 10.9 wt. % equiv. NaCl (Figs. 4 and 5).

Inclusions in stage I veins

Primary and pseudosecondary inclusions in stage I quartz homogenize at temperatures from 240° to 403°C. Homogenization temperature and salinity ranges of each inclusion type are as follows (Figs. 4 and 5): type Ia, 245°~369°C, 2.1~7.7 wt. %; type Ib, 251°~330°C, 2.6 wt. %; type II, 281°~357°C; type IIIa, 240°~403°C, 1.2~5.1 wt. %; type IIIb, 241°~331°C, 0.8~3.0 wt. % equiv. NaCl.

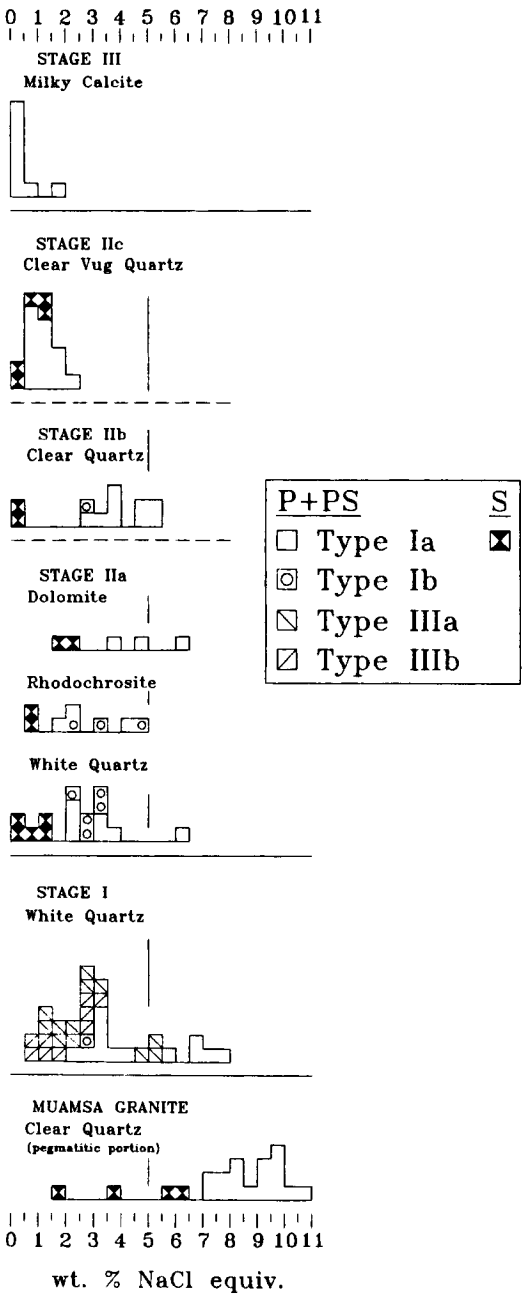

Fig. 5. Frequency diagrams of salinities of fluid inclusions in vein minerals from the Kwangsin mine, and in quartz from the Muamsa Granite.

Inclusions in stage II veins

Inclusions in substage IIa quartz homogenize at temperatures from 191° to 318°C and have salinities of 2.1 to 6.3 wt. % equiv. NaCl. Homogenization temperature and salinity ranges of each inclusion type are as follows (Figs. 4 and 5): type Ia, 191°~313°C, 2.1~6.3 wt. %; type Ib, 197°~303°C, 2.2~3.3 wt. % equiv. NaCl; type II, 233°~318°C. Rhodochrosite and dolomite from substage IIa veins contain type I and II inclusions whose homogenization temperature and salinity ranges are 252°~304°C and 1.6~6.1 wt. % equiv. NaCl.

Primary and pseudosecondary type I inclusions in substage IIb clear quartz homogenize at temperatures from 182° to 276°C and have salinities of 2.5 to 5.4 wt. % equiv. NaCl. Stage IIc clear vug quartz contains only type Ia inclusions which homogenize from 160° to 255°C and have salinities of 0.5 to 2.4 wt. % equiv. NaCl (Figs. 4 and 5).

Inclusions in stage III veins

Fluid inclusions in stage III calcite homogenize at lower temperatures ranging from 147° to 222°C and have salinities of 0.0 to 1.9 wt. % equiv. NaCl. Toward the wanning of hydrothermal activity, homogenization temperature and salinity of fluid inclusions become progressively lower to the level of about 100°C and 0.0 wt. % equiv. NaCl (Figs. 4 and 5). This indicates that progressive cooling and dilution of fluids occurred during the evolution of hydrothermal mineralization.

Variation in Temperature and Composition of Hydrothermal Fluids

Fluid inclusion data show that the hydrothermal fluids at Kwangsin compositionally belong to the H_2O-CO_2-NaCl system. The relationship between homogenization temperature and salinity of hydrothermal fluids (Fig. 6) indicates a complex history of boiling (accompanying CO_2 effervescence), cooling and dilution of ore fluids.

Vapor-rich type II inclusions occur in stage I and II minerals, but their salinity data cannot be obtained due to the small size (3~6 μm) of inclusions. They coexist with type I and III inclusions, indicating that stage I hydrothermal fluids were at or close to the boiling conditions. The occurrence of liquid CO_2-bearing (type III) inclusions with a wide range of CO_2/H_2O ratios may be related to the boiling of an H_2O-rich fluid containing minor amounts of dissolved CO_2, which could result in the separation of a vapor phase rich in

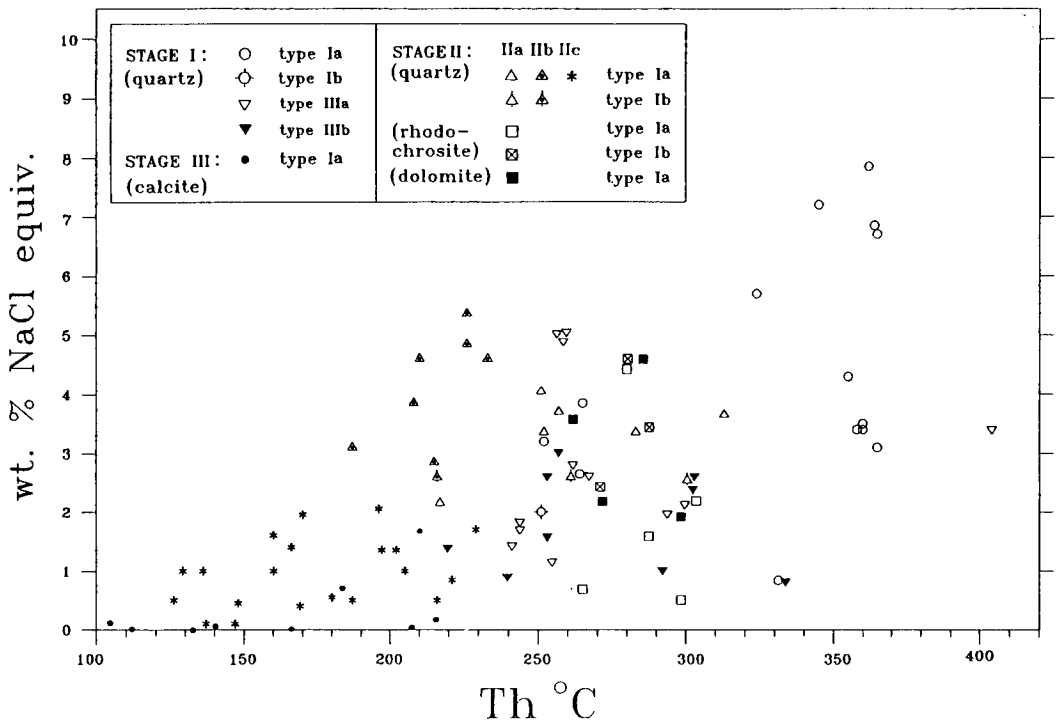

Fig. 6. Salinity versus homogenization temperature diag- ram for fluid inclusions in vein minerals from the Kwangsin mine.

Table 2. Compositional data of stage I fluid, determined by gas chromatographic analysis of the fluids extracted by crushing

Sample No.	H_2O mole%	CO_2 mole%	CH_4 mole%	N_2 mole%
K-6	96.50	1.99	0.43	0.18
K-8	98.40	1.32	0.30	0.00

CO_2. Therefore, the formation of type III inclusions was the result of continued boiling (down to about 250°C) and volatile segregation of CO_2-rich fluids. The separated, CO_2-rich fluids were progressively evolved and successively deposited stage II minerals (especially rhodochrosite). Measured and calculated compositions of liquid CO_2-bearing inclusions are summarized in Tables 2 and 3. Following the boiling, stage I fluid progressively cooled with increasing time (from about 350° to 250°C).

However, primary and pseudosecondary fluid inclusions (Th=280°~230°C), in stage IIb minerals display an increase of salinity (up to 5.4 wt. % equiv. NaCl), probably due to retrograde boiling of fluids (Fig. 6). This boiling might have resulted from the pressure decrease in response to fracturing of veins. Boiling in hydrothermal systems can result in abrupt changes in physicochemical environments of the fluids (e.g., temperature, pH, oxygen fugacity, ΣH_2S, ΣCO_2; Drummond, Ohmoto, 1985). These changes, especially both the drops in temperature and f_{H2S} and the increase in pH favour deposition of base-metal sulfides through destabilization of metal chloride and/or sulfide complexes (Steven, Eaton, 1975; Berger, Eimon, 1983; Reed, Spycher, 1986). There- fore, we interpret the deposition of early sulfides as the result of fluid boiling. However, later mixing of fluids resulted in a linear correlation between homogenization temperature and salinity (Fig. 6). Such a mixing occurred likely due to further fracturing of veins, allowing the inundation of cooler ($\leq$ 100°C) and more dilute (0.0 wt. % equiv. NaCl) meteoric groundwaters in the hydrothermal system.

We consider that base-metal deposition at Kwangsin was a combined result of boiling and later meteoric water mixing.

Pressure-Depth Consideration

Vapor-rich (type II) inclusions are associated with

Table 3. Microthermometric data of liquid CO_2-bearing (type III) inclusions in stage I quartz from the Kwangsin deposit

Type	Tm_{CO2} (°C)	Tm_{clath} (°C)	Th_{CO2} (°C)	Th_{total} (°C)	vol. % aq[1]	density (g/cc)[2]			wt. % NaCl equiv.	X_{CO2}	X_{H2O}	X_{NaCl}
						CO_2	H_2O	total				
IIIa	-57.0	9.1	31.1	247	5	0.51	1.00	0.54	1.8	0.80	0.20	0.00
	-56.6	9.1	31.1	246	10	0.52	1.00	0.56	1.8	0.66	0.34	0.00
	-56.6	9.3	31.0	241	5	0.52	1.00	0.54	1.4	0.89	0.20	0.00
	-57.0	8.3	28.3	403	30	0.65	1.01	0.76	3.4	0.39	0.61	0.00
	-56.7	9.0	26.3 (V)	294	40	0.26	1.00	0.56	2.0	0.14	0.86	0.01
	-56.6	9.4	18.6	255	30	0.79	1.00	0.85	1.2	0.57	0.43	0.00
	-56.9	7.4	20.7	256	30	0.77	1.03	0.85	5.1	0.42	0.57	0.01
	-56.9	7.5	19.8	257	50	0.78	1.03	0.90	4.9	0.24	0.75	0.01
	-57.4	8.7	21.1	266	80	0.76	1.01	0.96	2.6	0.70	0.92	0.01
	-56.9	7.4	16.6	258	70	0.81	1.03	0.96	5.1	0.13	0.86	0.01
	-56.9	8.6	21.1	261	50	0.76	1.01	0.89	2.8	0.24	0.75	0.01
	-56.6	8.9	29.9	300	85	0.60	1.01	0.95	2.2	0.04	0.95	0.01
IIIb	-56.6	9.2	31.0	253	10	0.52	1.00	0.57	1.6	0.66	0.34	0.00
	-56.6	9.5	28.3	292	30	0.65	1.00	0.75	1.0	0.39	0.61	0.00
	-57.0	8.7	30.2	303	20	0.59	1.01	0.67	2.6	0.49	0.50	0.00
	-57.5	8.5	30.2	258	20	0.59	1.01	0.67	3.0	0.49	0.50	0.00
	-57.5	8.7	30.5	254	20	0.57	1.01	0.66	2.6	0.49	0.51	0.00
	-56.9	9.6	16.4	240	50	0.81	1.00	0.90	0.8	0.25	0.75	0.00
	-56.7	8.7	29.9	302	50	0.60	1.01	0.80	2.6	0.20	0.79	0.01
	-57.0	9.3	26.0	270	40	0.70	1.00	0.82	1.4	0.30	0.70	0.00
	-57.2	9.6	28.3	331	35	0.65	1.00	0.77	0.8	0.33	0.67	0.00

[1]Visual estimate at room temperature; [2]Based on homogenization temperature of CO_2 phase (Th_{CO2}) and the mode of homogenization (Bodnar *et al.*, 1985; Parry, 1986). Abbreviations: aq; aqueous phase, clath; CO_2 clathrate, Tm; melting temperature, Th; homogenization temperature.

aqueous liquid-rich inclusions (type I) in stage I and IIa quartz (largely prior to main Pb-Zn mineralization), and homogenize at the temperatures of 230° to 360°C (Figs. 4 and 6). This fact indicates that boiling of ore fluid possibly occurred prior to and/or during the main ore mineralization. No pressure corrections are necessary for these inclusions.

Data for the H_2O-NaCl system (Sourirajan, Kennedy, 1962; Haas, 1971), combined with temperature (> 270° to 360°C; except one fluid inclusion with the homogenization temperature of ≈230°C) and salinity (probably < 5 wt. % equiv. NaCl) data for fluid inclusions, indicate that ore fluids trapped in pressures of about 170 to 55 bars. These pressures correspond to approximate maximum depths of 2200 to 600 m and 700 to 200 m, assuming hydrostatic and lithostatic pressure regimes, respectively. Massive appearance of stage I and IIa veins may indicate that pressure regime was dominantly lithostatic. A recognized salinity increase in fluid inclusions from stage IIb minerals also may be explained by the boiling. However, characteristic vein textures of stage IIb veins (including vuggy nature) may indicate that the veins were opened to the atmosphere during the stage IIb mineralization. Assuming that the pressure regime was changed from dominantly lithostatic (during stage I and IIa mineralization) to hydrostatic (during stage IIb mineralization) conditions, the depths of hydrothermal mineralization at Kwangsin was constant around 600~700 m from the paleo-surface.

GEOCHEMICAL CONDITIONS OF MINERALIZATION

Ranges of temperature and fugacity of sulfur (fs_2) for the stage II fluids were estimated from the phase relations and mineral compositions in the systems Fe-As-S (Kretschmar, Scott, 1976), Fe-Zn-S (Barton, Toulmin, 1966), Fe-S (Helgeson, 1969), and Au-Ag-S (Barton, Toulmin, 1964), as shown in Fig. 7.

For the stage IIa mineralization (prior to the main Pb-Zn deposition), the pyrite+arsenopyrite (29.5~30.6 atom. % As)+sphalerite (14.8~16.0 mole % FeS) assemblage indicates the temperature and log fs_2 conditions of 280° to 350°C and -11.4 to -8.7 atm, respectively (Fig. 7).

During the main Pb-Zn deposition (stage IIb), the occurrence of pyrite+sphalerite (8.2~13.1 mole % FeS) +galena+argentite assemblage indicates the approximate log fs_2 values of -15.5 to -11.8 atm at temperatures of 200° to 260°C (Kretschmar, Scott, 1976). The lower limit of log fs_2 values was set by the FeS content of sphalerite and argentite-native silver reaction curve; the upper limit was set by the FeS content of

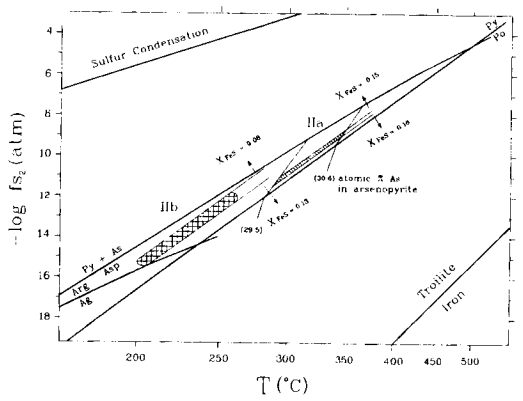

Fig. 7. Fugacity of sulfur versus temperature diagram showing the depositional conditions of stage II mineralization at the Kwangsin mine. Hatched and cross-hatched areas represent depositional conditions of substage IIa (pyrite+arsenopyrite+sphalerite) and substage IIb (pyrite+sphalerite+galena+argentite) mineral assemblages, respectively. Compositional isopleths for sphalerite (mole % FeS, X_{FeS}) and arsenopyrite are from Barton, Toulmin (1966) and Kretschmar, Scott (1976), respectively. Abbreviations: Ag=native silver, Arg=argentite, As=native arsenic, Asp=arsenopyrite, Po=pyrrhotite, Py=pyrite.

sphalerite and the homogenization temperature of fluid inclusions. It is impossible to define the fs_2 condition for the stage IIc mineralization in vugs, due to the lack of suitable mineral assemblages. Fig. 7 shows the general decrease in the fs_2 and temperature conditions during stage II mineralization.

STABLE ISOTOPE STUDIES

In this study we measured the sulfur isotope composition of sulfides, carbon isotope composition of vein carbonates (rhodochrosite, dolomite and calcite), oxygen isotope composition of vein minerals (quartz, calcite, rhodochrosite and dolomite) and granite (quartz and potassium feldspar from pegmatitic portions of the Muamsa Granite), hydrogen isotope composition of inclusion waters from vein minerals. Standard techniques for extraction and analysis were used as described by McCrea (1950), Grinenko (1962), Taylor, Epstein (1962), and Hall, Friedman (1963). Isotope data are reported in standard δ notation relative to the Canyon Diablo troilite (CDT) standard for S, the Pee Dee belemnite (PDB) standard for C, and the Vienna SMOW standard for O and H. The standard error of each analysis is approximately ±0.1 per mil for C, O and S, and ±2 per mil for H.

Sulfur Isotope Study

Table 4. Sulfur isotope data of sulfides from the Kwangsin Pb-Zn deposit

Sample No.	Stage	Mineral	$\delta^{34}S$ (‰)	$\Delta^{34}S$ (‰)	T (°C)[1]	T (°C)[2]	$\delta^{34}S_{H2S}$ (‰)[3]
K-10	IIa	py	14.5			280	13.2
K-24	IIa	py	13.9			280	12.6
K-1	IIb	sp	11.7				11.3
				sp-gn 2.7	244±20		
K-1	IIb	gn	9.0				11.3
K-12	IIb	gn	11.6			250	13.9
K-14	IIb	py	12.9			220	11.3
K-18	IIb	sp	11.9			220	11.5
K-4	IIc	gn	10.7			200	13.5
L-93-1	IIc	sp	13.2			180	12.7
K-94-3	IIc	py	14.5			190	12.6

[1] Sulfur isotope temperature based on sulfur isotope fractionation equation compiled by Ohmoto, Rye (1979); [2]Based on average fluid inclusion homogenization temperatures and paragenetic constraints; [3]Based on sulfur isotope fractionation equations compiled by Ohmoto, Rye (1979). Abbreviations: gn; galena, sp; sphalerite, py; pyrite.

Sulfur isotope data were obtained for 10 hand-picked sulfides (4 pyrites, 3 sphalerites, 3 galenas) from stage II veins. The $\delta^{34}S$ values range from 9.0 to 14.5 ‰ (Table 4). One sphalerite-galena pair has a $\Delta^{34}S$ value of 2.7 ‰, yielding an apparent equilibrium temperature of 244±20°C (Table 4).

Based on the fluid inclusion homogenization temperatures, $\delta^{34}S$ values of H_2S in stage II fluids were calculated to fall in the range of 11.3 to 13.9 per mil (Table 4; Fig. 8). The calculated $\delta^{34}S_{H2S}$ values show small variations over a temperature range of 280° to 180°C, indicating the dominance of H_2S in the ore fluids, as a temperature decrease (up to 100°C) would have little effect on the $\delta^{34}S_{H2S}$ values of a fluid if its sulfur were dominantly H_2S (Ohmoto, Rye, 1979).

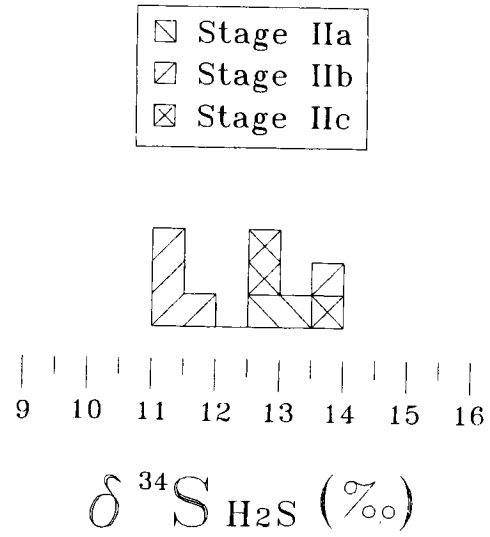

Fig. 8. Sulfur isotope composition of H_2S in equilibrium with hydrothermal vein sulfides from the Kwangsin mine.

Therefore, the $\delta^{34}S_{H2S}$ values (11.3 to 13.9 ‰) may be taken as an approximation of the sulfur isotope composition of the entire solution ($\delta^{34}S_{\Sigma S}$). It is interesting that the $\delta^{34}S_{\Sigma S}$ values are quitely higher than those for most igneous sources of sulfur ($\delta^{34}S_{\Sigma S}$ values about of 0 to 5 ‰; Ohmoto, Rye, 1979; Field, Fifarek, 1986). To our knowledge, the $\delta^{34}S_{H2S}$ values of > 10 ‰ have not been recognized from hydro- thermal metallic ore deposits in Korea. These $\delta^{34}S_{H2S}$ values for the Kwangsin ore fluids may indicate that an igneous source of sulfur (likely from the nearby Muamsa Granite) largely mixed with an isotopically heavier source (with an $\delta^{34}S_{\Sigma S}$ value of > 13 ‰) of sulfur (possibly the sulfates in clastic sedimentary rocks) during the mineralization (So, Yun, 1992).

Carbon, Oxygen and Hydrogen Isotope Study

The $\delta^{13}C$, $\delta^{18}O$ and δD values for examined minerals and their inclusion fluids are summarized in Table 5. Carbonate minerals (1 rhodochrosite, 1 dolomite and 3 calcites) from stage II and III veins have $\delta^{13}C$ values of +1.0 to -5.0‰. Coupled with fluid inclusion homogenization temperatures, the calcite-CO_2 carbon isotope fractionation of calcite (Friedman, O'Neil, 1977) yields the $\delta^{13}C_{CO2}$ values between -1.9 and -4.0 per mil, possibly indicating a deep igneous source of carbon (Pineau *et al.*, 1976; Field, Fifarek, 1986).

Measured $\delta^{18}O$ values of carbonates are as follows (Table 5): 8.4‰ for rhodochrosite; 13.8‰ for dolomite; 9.5 to 8.7‰ for calcite. Using the calcite-water (O'Neil *et al.*, 1969) and dolomite-water (Matthews, Katz, 1977) oxygen isotope fractionation equations, coupled with temperature estimates based on fluid inclusions, and paragenetic constraints, the $\delta^{18}O$ values

Table 5. Carbon, oxygen, and hydrogen isotope data from the Kwangsin Pb-Zn deposit

Sample No.	Stage	Mineral	$\delta^{13}C$ (‰)	$\delta^{18}O$ (‰)		T (°C)[1]	$\delta^{18}O_{water}$ (‰)[2]	δD_{water} (‰)[3]
K-8-1	I	qz		19.4		280	11.8	-51
K-19	I	qz		21.1		310	14.6	
K-1	I	qz		17.0		300	10.1	-69
K-24	IIa	rhodo	-5.0	8.4		280	2.2	-73
K-93-2	IIa	do	+1.0	13.8		260	5.8	
K-12	IIb	qz		10.0		244[4]	0.8	-76
K-14	IIb	qz		8.4		220	-2.0	
K-18	IIc	vug qz		5.1		195	-6.8	
K-24	IIc	vug qz		5.8		195	-6.1	
K-25	IIc	vug qz		5.6		195	-6.3	
K-8-2	III	cc	-3.0	9.5		180	-1.2	-83
K-8	III	cc	-3.3	8.7		160	-3.2	-85
K-14	III	cc	-1.2	9.3		160	-2.6	-82
MG-1		qz		9.5			5.4	
					qz-K-fd	396[5]		
MG-1		K-fd		8.2			5.4	
GS-861[6]		qz		9.7			5.9	
					qz-K-fd	414[5]		
GS-861[6]		K-fd		8.7			5.9	
GS-867[6]		qz		10.0		400	6.5	
YS-23[7]		qz		9.8		400	5.7	

[1]Based on average fluid inclusion temperatures and paragenetic constraints; [2]Based on oxygen isotope fractionation factors: quartz-water, Matsuhisa *et al.* (1979); calcite-water, O'Neil *et al.* (1969); dolomite-water, Matthews, Katz (1977); [3]Hydrogen isotope composition of water in inclusion fluids (extracted by crushing); [4]Based on calculated sulfur isotope temperatures; [5]Based on oxygen isotopic fractionation equation of Matsuhisa *et al.* (1979); [6]Data from So, Yun (1992); [7]Data from Kim, Shin (1990). Abbreviations: qz; quartz, cc; calcite, do; dolomite, K-fd; K-feldspar, rhodo; rhodochrosite.

of water in equilibrium with carbonates are as follows: 2.2‰ for rhodochrosite; 5.8‰ for dolomite; -1.2 to -3.2‰ for calcite. For this calculation, the oxygen isotope fractionation between rhodochrosite and water was assumed to be same with that between calcite and water. The $\delta^{18}O$ values of vein quartzes from several stages are as follows (Table 5): 21.1 to 17.0‰ for stage I; 10.0 to 8.4‰ for stage IIb; 5.8 to 5.1‰ for stage IIc. Using the quartz-water oxygen isotope fractionation equation of Matsuhisa *et al.* (1979), the oxygen isotope compositions of waters in hydrothermal fluids are calculated as follows (Table 5): stage I, 14.6 to 10.1‰; stage IIb, 0.8 to -2.0‰; stage IIc, -6.1 to -6.8‰; stage III, -1.2 to -3.2‰.

Fluid inclusion waters were extracted by crushing from vein quartz and carbonate samples and analyzed for hydrogen isotope composition. The δD values of inclusion waters are as follows (Table 5): stage I, -51 to -69‰; stage IIa, -73‰; stage IIb, -76‰; stage III, -82 to -85‰.

Interpretation of Oxygen and Hydrogen Isotope Results

The calculated $\delta^{18}O_{water}$ values show a systematic decrease with increasing paragenetic time and decreasing temperature, from 14.6 to 10.1‰ for stage I, through 5.8 to 2.2‰ for stage IIa and 0.8 to -2.0‰ for stage IIb, to -6.1 to -6.8‰ for stage IIc (Table 5; Fig. 9). This trend indicates an overall progressive increase of meteoric water influx in the hydrothermal system.

Fig. 10 shows the distribution of measured and calculated hydrothermal fluid compositions on a conventional H versus O isotope diagram. The $\delta^{18}O_{water}$ data from stage I quartz likely represent the meteoric water whose isotopic composition was shifted greatly by the exchange with a large volume of metamorphic (or metasedimentary) and sedimentary rocks at high temperatures, because measured δD values seem to overlap the range of metamorphic waters. The $\delta^{18}O_{water}$ and δD_{water} data from the stage II and stage III minerals fall toward the meteoric water line, indicating the mixing of highly exchanged meteoric water with less exchanged meteoric water or unexchanged meteoric water.

We conclude that Kwangsin Pb-Zn deposit formed from meteoric water-derived hydrothermal fluids whose isotopic compositions were controlled by the interaction with the Samtaesan Formation ($\delta^{18}O$=20.1 to 24.9‰; Kim, 1984; So *et al.*, 1983), the Suchangni

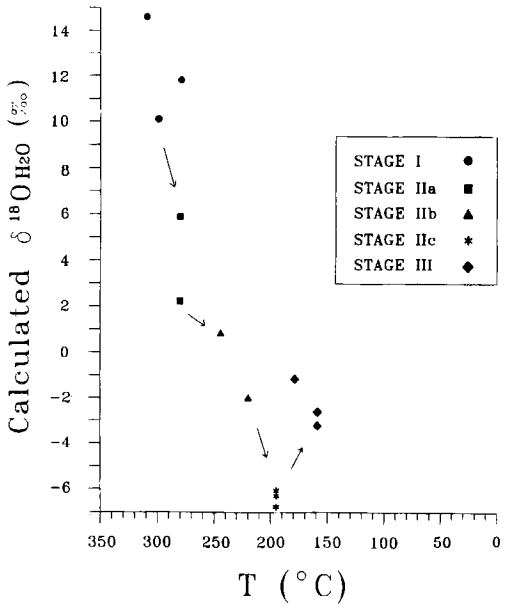

Fig. 9. Temperature versus oxygen isotope diagram displaying the systematic decrease of $\delta^{18}O$ valu es of water in the Kwangsin hydrothermal fluids with increasing paragenetic time.

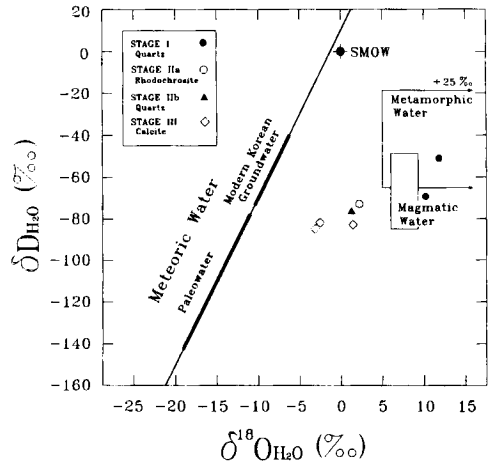

Fig. 10. Hydrogen versus oxygen isotope diagram, displaying stable isotope systematics of hydrothermal fluids from the Kwangsin mine. The magmatic and metamorphic water boxes (Taylor, 1974, 1979) and the meteoric water line (Craig, 1961) are also shown. The range of the Korean paleometeoric water composition is from Shelton *et al.* (1988) and So *et al.* (1990). The compositional range of modern Korean groundwaters is from Kim, Nakai (1988).

Formation and/or the Muamsa Granite ($\delta^{18}O \approx 9‰$, So, Yun, 1992) under low water-to-rock ratios.

SUMMARY

Based on preceding discussions of geologic, mineralogical, fluid inclusion, and stable isotope data, the following genetic model is proposed for the Kwangsin Pb-Zn deposit.

1. The Kwangsin Pb-Zn deposit was formed in three stages of quartz and carbonates veins that filled fault-related fractures in the Samtaesan Formation. The mineralization occurred during Late Cretaceous (83.5 Ma), genetically in relation to the cooling history of the nearby Muamsa Granite (83~87 Ma).

2. Mineral assemblages, fluid inclusions, and sulfur isotope data indicate that Pb-Zn deposition in stage IIb occurred mostly at temperatures of 182° to 276°C from fluids with salinities between 2.7 and 5.4 wt. % equiv. NaCl. The Pb-Zn deposition was a result of fluid boiling and later meteoric water mixing at depths between 600 and 700 m. The ore-forming fluids of stage IIb had log fs_2 values of -15.5 to -11.8 atm.

3. Calculated $\delta^{34}S_{\Sigma S}$ values of ore fluids are quitely high (11.3 to 13.9‰), and indicate that an igneous source of sulfur largely mixed with an isotopically heavier sulfur source (sedimentary sulfates ?). Measured and calculated hydrogen and oxygen isotope compositions of waters indicate that the hydrothermal system at Kwangsin formed from a deeply circulating meteoric waters which evolved through interaction with nearby sedimentary and/or metasedimentary rocks (including the Samtaesan Formation with $\delta^{18}O$ values of 20.1 to 24.9‰) under low water-to-rock ratios. A systematic decrease in calculated $\delta^{18}O_{water}$ value with increasing paragenetic time (and decreasing temperature) indicates a progressively increasing amounts of meteoric water influx in the hydrothermal system.

ACKNOWLEDGEMENTS

This research was financially supported by the funds from the Center for Mineral Resources Research (CMR) and the Korean Ministry of Education (through 1996 Research Fund to Yun, S. T.; No. BSRI-96-5422). Stable isotope analyses were performed in the laboratories of Prof. Shelton, K. L. (Univ. Missouri-Columbia). We acknowledge Prof. Kim, K. H. (Ewha Woman's University) for helpful suggestions to the manuscript.

REFERENCES

Barton, P.B., Jr. and Toulmin, P., III (1964) The electrum tarnish method for determination of the fugacity of sulfur in laboratory sulfide systems. Geochim. Cosmochim. Acta,

v. 28, p. 619-640.

Barton, P.B., Jr. and Toulmin, P., III (1966) Phase relations involving sphalerite in the Fe-Zn-S system. Econ Geol., v. 61, p. 815-849.

Berger, B.R. and Eimon, P. (1983) Conceptual models of epithermal precious-metal deposits, in Shanks, W.C., III, ed, Cameron Volume on Unconventional Mineral Deposits. Society of Mining Engineers, American Institute of Mining and Metallurgy, p. 292-302.

Bodnar, R.J. (1993) Revised equation and table for determining the freezing point depression of H2O-NaCl solutions. Geochim. Cosmochim. Acta, v. 57, p. 683-684.

Bodnar, R.J., Reynolds, T.J. and Kuehn, C.A. (1985) Fluid inclusion systematics in epithermal systems. Rev. Econ. Geol,. Volume 2, p. 73-97.

Bozzo, A.T., Chen, H.S., Kaas, J.R. and Barduhn, A.J. (1975) The properties of hydrates of chlorine and carbon dioxide. Desalination, v. 16, p. 303-320.

Craig, H. (1961) Isotopic variations in meteoric waters. Science, v. 133, p. 1702-1703.

Diamond, L.W. (1992) Stability of CO_2 clathrate hydrate+CO_2 liquid+CO_2 vapour+aqueous KCl-NaCl solutions. Experimental determination and application to salinity estimations of fluid inclusions. Geochim. Cosmochim. Acta, v. 56, p. 273-280.

Drummond, S.E. and Ohmoto, H. (1985) Chemical evolution and mineral deposition in boiling hydrothermal system. Econ. Geol., v. 80, p. 126-147.

Field, C.W. and Fifarek, R.H. (1986) Light stable-isotope systematics in the epithermal environment. Rev. Econ. Geol., Volume 2, p. 99-128.

Friedman, I. and O'Neil, J.R. (1977) Compilation of stable isotope fractionation factors of geochemical interest, in Fleisher, M., ed., Data of geochemistry, Sixth Edition, U.S. G.S. Prof. Paper 440-KK. p. KK4-KK12.

Grinenko, V.A. (1962) Preparation of sulfur dioxide for isotopic analysis. Zeitschr. Neorgan. Khimii, v. 7, p. 2478-2483.

Haas, J.L., Jr. (1971) The effect of salinity on the maximum thermal gradient of a hydrothermal system at hydrostatic pressure. Econ. Geol., v. 66, p. 940-946.

Hall, W.E. and Friedman, I. (1963) Composition of fluid inclusions, Cave-in-Rock fluorite district, Illinois and Upper Mississippi Valley zinc-lead district. Econ. Geol., v. 58, p. 886-911.

Hedenquist, J.W. and Henley, R.W. (1985) The importance of CO_2 on freezing point measurements of fluid inclusions: Evidence from active geothermal systems and implications for epithermal ore deposition. Econ. Geol., v. 80, p. 1379-1406.

Helgeson, H.C. (1969) Thermodynamics of hydrothermal systems at elevated temperatures and pressures. Am. Jour. Sci., v. 267, p. 729-804.

Kim, K.H. (1984) Isotopic ratios of carbon and oxygen in some limestones in South Korea. Ewha Womans University [Seoul], Korean Research Institute of Better Living Journal, v. 35, p. 133-142 (in Korean).

Kim, K.H. and Nakai, N. (1988) Isotopic compositions of precipitations and groundwaters in South Korea. Geol. Soc. Korea Jour., v. 24, p. 37-46 (in Korean).

Kim, K.H. and Shin, Y.S. (1990) Petrochemistry of the granitic rocks in the Chungju, Wolagsan and Jecheon granite batholiths. Korean Inst. Mining Geology Jour., v. 23, p. 245-259 (in Korean).

Kim, K.W., Park, B.S. and Lee, H.K. (1967) Explanatory text of the geological map of Jecheon sheet. Geol. Surv. of Korea, 46P.

Kim, S.E. and Kim, S.Y. (1980) The study of geology and ore deposits of mine claim No. 17 in Jecheon sheet.

Kretschmar, U. and Scott, S.D. (1976) Phase relations involving arsenopyrite in the system Fe-As-S and their application. Canadian Mineralogist, v. 14, p. 364-386.

Matsuhisa, Y., Goldsmith, J.R. and Clayton, R.N. (1979) Oxygen isotopic fractionation in the system quartz-albite-anorthite-water. Geochim. Cosmochim. Acta, v. 43, p. 1131-1140.

Matthews, A. and Katz, A. (1977) Oxygen isotope fractionation during dolomitization of calcium carbonate. Geochim. Cosmochim. Acta, v. 41, p. 1431-1438.

McCrea, J.M. (1950) The isotope chemistry of carbonates and a paleotemperature scale. Jour. Chem. Physics, v. 18, p. 849-857.

Ohmoto, H. and Rye, R.O. (1979) Isotopes of sulfur and carbon, in Barnes, H.L., ed., Geochemistry of hydrothermal ore deposits. New York, Wiley Intersci., p. 509-567.

O'Neil, J.R., Clayton, R.N. and Mayeda, T.K. (1969) Oxygen isotope fractionation in divalent metal carbonates. Journal of Chemical Physics, v. 51, p. 5547-5558.

Parry, W.T. (1986) Estimation of X_{CO_2}, P and fluid inclusion volume from fluid inclusion temperature measurements in the system NaCl-CO_2-H_2O. Econ. Geol., v. 81, p. 1009-1013.

Pineau, F., Javoy, M. and Bottinga, Y. (1976) $^{13}C/^{12}C$ ratios of rocks and inclusions in popping rocks of the Mid-Atlantic Ridge and their bearing on the problem of isotopic composition of deep-seated carbon. Earth Planet Sci. Letters, v. 29, p. 413-421.

Reed, M.H. and Spycher, N.F. (1986) Boiling, cooling and oxidation in epithermal systems. A numerical modeling approach, in Berger, B.R. and Bethke, P.M, ed, Geology and geochemistry of epithermal systems. Rev. Econ. Geol., Volume 2, p. 249-272.

Shelton, K.L., So, C.S. and Chang, J.S. (1988) Gold-rich mesothermal vein deposits of the Republic of Korea: Geochemical studies of the Jungwon gold area. Econ. Geol., v. 83, p. 1221-1237.

So, C.S., Rye, D.M. and Shelton, K.L. (1983) Carbon, hydrogen, oxygen and sulfur isotope and fluid inclusion study of the Weolag tungsten-molybdenum deposit, Republic of Korea: Fluid histories of metamorphic and ore-forming events. Econ. Geol., v. 78, p. 1551-1573.

So, C.S. and Yun, S.T. (1992) Geochemistry and genesis of hydrothermal Au-Ag-Pb-Zn deposits in the Hwanggangri mineralized district, Republic of Korea. Econ. Geol., v. 87, p. 2056-2084.

So, C.S., Yun, S.T., Chi, S.J. and Choi, S.H. (1990) Geochemical studies of hydrothermal gold-silver deposits, Republic of Korea: Chilgok area. Neues Jahrb. Mineralogie Abh., v. 161, p. 79-99.

Sourirajan, S. and Kennedy, G.C. (1962) The system H_2O-NaCl at elevated temperatures and pressures. Am. Jour.

Sci., v. 260, p. 115-141.

Steven, T.A. and Eaton, G.P. (1975) Environment of ore deposition in the Creede mining district, San Juan Mouentains, Colorado: I. Geologic, hydrologic, and geophysical setting. Econ. Geol., v. 70, p. 1023-1037.

Taylor, H.P., Jr. (1974) The application of oxygen and hydrogen isotope studies to problems of hydrothermal alteration and ore deposition. Econ. Geol., v. 69, p. 843-883.

Taylor, H.P., Jr. (1979) Oxygen and hydrogen isotope relations in hydrothermal ore deposits, in Barnes, H.L., ed., Geochemistry of hydrothermal ore deposits. New York, Wiley Intersci., p. 236-277.

Taylor, H.P., Jr. and Epstein, S. (1962) Relationship between $^{18}O/^{16}O$ ratios in coexisting minerals in igneous and metamorphic rocks - Part I. Principles and experimental results. Geol. Soc. Am. Bull., v. 73, p. 461-480.

Manuscript received 27 October 1997

광신 연-아연 광상의 유체포유물 및 안정동위원소 연구

최광준 · 윤성택 · 소칠섭

요 약 : 광신 연-아연 광산은 단층 열극을 충진한 열극 충진 광상으로서 조선계의 삼태산층과 시대미상의 서창리층에 발달된 석영과 탄산염맥으로 이루어져 있다. 광화작용은 3회에 걸쳐 진행되었으며, 각 광화시기의 특징은 다음과 같다. 광화 I기=barren한 석영의 침전기, 광화 II기=석영과 능망간석에 수반된 연-아연 광물의 주 침전기, 광화 III기=barren한 방해석의 침전기. 특히, 연-아연 광물은 주로 광화 IIb기에 침전하였다. 유체포유물 연구에 의하면, 광화 IIb기 광화유체의 온도와 염농도는 182°~276℃와 2.7~5.4 wt. % NaCl 상당 염농도였으며, 연-아연 광물의 침전은 주로 비등작용과 더불어 후기의 천수 혼입작용에 기인하였음을 지시한다. 광화작용은 약 600~700 m의 심도에서 이루어진 것으로 판단된다. 섬아연석과 유비철석의 성분 함량을 이용하여 추정한 광화 IIb기의 황분압 ($\log fs_2$)은 -15.5~-11.8 atm이다. 황화물의 황동위원소 조성 ($\delta^{34}S_{CDT}$=9.0~14.5 ‰)에 근거한 열수유체의 전(全) 황동위원소값 ($\delta^{34}S_{\Sigma S}$)은 약 14 ‰로서 매우 높은데, 이는 심부 화성기원의 황이 퇴적암류내의 황산염과 다소 혼합된 결과로 사료된다. 산소-수소 동위원소 분석 연구에 의하면, 광화유체는 낮은 수-암비 환경 하에서 주로 주변 모암인 삼태산층 ($\delta^{18}O$=20.1~24.9 ‰)과 상당히 반응한 심부 순환 천수로부터 형성되었다. 한편, 광화유체의 산소동위원소값 ($\delta^{18}O_{H2O}$)은 광화작용의 진행과 더불어 체계적으로 감소 (광화 I기, 14.6~10.1 ‰; 광화 IIa기, 5.8~2.2 ‰; 광화 IIb기, 0.8~-2.0 ‰; 광화 IIc기, -6.1~-6.8 ‰)하였다. 이는 열수계 내로의 천수 혼입이 시간 경과와 더불어 점진적으로 증가하였음을 지시한다.